Vesuvianite from Somma-Vesuvius volcano (southern Italy): chemical, X-ray diffraction and single-crystal polarized FTIR investigations

Giuseppina Balassone[1,*], Dominik Talla[2,3], Anton Beran[2], Angela Mormone[4],
Angela Altomare[5], Anna Moliterni[5], Nicola Mondillo[1], Michele Saviano[5] and Carmela Petti[6]

[1] Dipartimento di Scienze della Terra, Università degli Studi di Napoli Federico II,
Via Mezzocannone 8, 80134 Napoli, Italy
[2] Institut für Mineralogie und Kristallographie, Geozentrum Universität Wien,
Althanstrasse 14, A-1090 Wien, Austria
[3] Department of Geological Sciences, Masaryk University, Kotlarska 2, 61137 Brno, Czech Republic
[4] Osservatorio Vesuviano, INGV, Via Diocleziano, 80124 Napoli, Italy
[5] Istituto di Cristallografia, CNR, Via Giovanni Amendola, 122/o, 70126 Bari, Italy
[6] Centro Museale 'Centro Musei delle Scienze Naturali', Università degli Studi di Napoli Federico II,
Via Mezzocannone 8, 80134 Napoli, Italy
*Corresponding author: *balasson@unina.it*

Abstract

A suite of twelve vesuviante samples from skarn and syenitc ejecta from the Somma-Vesuvius volcanic complex was studied by means of a combination of energy dispersive spectrometry (EDS), inductively-coupled plasma-mass spectrometry (ICP-MS), powder and single-crystal X-ray diffraction, polarized radiation Fourier-transform infrared (FTIR) single-crystal micro-spectrometry. Some thermo-gravimetric analyses (TGA) were also performed. Vesuvianite crystals are dark brown to honey yellow-brown, rarely reddish-brown, and up to 2 centimetres in dimension. Their major elements (SiO_2, Al_2O_3, CaO and MgO) composition is rather constant, while Fe_2O_3, MnO and TiO_2 are slightly more variable. Light elements (B, Be and Li), Y, REE and actinides (Th, U) have been detected in all samples in minor to trace amounts, together with V, Zn, Zr, Sn, Co, Ga, Nb, Ta, Hf, Pb and Bi. Among the volatiles, fluorine is prevailing (in a range 1.41-2.25 wt. %). Water and chlorine are always observed, in the range 0.67-1.03 wt. % and 0.01-0.05 wt. %, respectively. Single-crystal X-ray diffraction analyses of vesuvianite gave *P*4/*nnc* as the most probable space group. Cell parameters vary from 15.542 Å up to 15.576 Å for *a* and 11.800 Å up to 11.827 Å for *c*. Polarized FTIR spectra of the OH fundamental measured parallel to the *c*-axis are dominated by absorption bands at 3638, 3567, 3452 and 3200 cm^{-1}, with two additional bands centred at 3590 and 3117 cm^{-1}. All bands show strong pleochroism with maximum absorption parallel to the *c*-axis and weak absorption components perpendicular to *c*. The spectra measured perpendicular to the *c*-axis are also dominated by the 3567, 3590 and 3638 cm^{-1} band group. OH amounts have been calculated using the total integrated absorption coefficient derived from the fitted spectra.

These contents are in good agreement with the H_2O values obtained by TGA. The formation temperature and the chemical environment of vesuvianite point to at least 800-890 °C and to the occurrence of chloride-fluoride-sulfate-carbonate-rich saline fluids, which are also rich in incompatible elements.

Key words: vesuvianite; Somma-Vesuvius volcano; ejecta; chemical analyses; X-ray diffraction; FTIR spectroscopy.

Introduction

Vesuvianite is a fairly common rock-forming or accessory Ca, Al, Fe, Mg-bearing silicate found in a wide range of occurrences, like thermally metamorphosed limestones or metasomatic rocks (hornfels, skarns), in regional metamorphosed calc-silicate rocks, in rodingites and metarodingites, in metasomatized silica-undersaturated nepheline syenites (Gnos and Armbruster, 2006). Due to its abyssophobic feature (Galuskin et al., 2007a), it is normally not observed in high-pressure environments, like blueschist- or eclogite-facies rocks, even if some occurrence in jadeitites from Guatemala and Myanmar have been recently decribed (Nyunt et al., 2009 and references therein).

The vesuvianite group consists of four varieties, i.e. vesuvianite (Mg, OH-rich), wiluite (B-rich) manganvesuvianite and fluorvesuvianite (Warren and Modell, 1931; Arem and Burnham, 1969; Coda et al., 1970; Rucklidge et al., 1975; Groat et al., 1992a, b, 1998; Armbruster and Gnos, 2000a; Armbruster et al., 2002; Britvin et al., 2003, Bellatreccia et al., 2005a). This mineral group is characteristic for its extremely complex chemical composition, manifold exchange mechanisms and cation ordering, the latter responsible for deviations from the *P*4/*nnc* symmetry and for typical polytypic arrangements (Elmi et al., 2011).

At the Somma-Vesuvius volcanic complex (Campania region, southern Italy), the type locality (Ciriotti et al., 2009), vesuvianite is one of the typical skarn minerals of many ejected rocks commonly associated with Plinian and sub-Plinian eruptions (Gilg et al., 2001). It is also quite commonly recorded in some syenitic (the so-called vesuvian "sanidinites") ejecta, rocks of particular interest to mineralogists due to the frequent occurrence of exotic minerals especially containing incompatible elements, like Zr-Ti-Th-U-REE (Della Ventura et al., 1996; 1999; Bellatreccia et al., 2002).

First described by Kappeler (1723) and then named vesuviante by Werner (1795), the vesuvianite samples show fairly variable appearance, as both color (black, reddish-brown, greenish-brown, dark brown, yellow-green or transparent greenish-yellow) and crystal habit, which can be prismatic, more or less striated with a square cross-section, short and thick columnar, bipyramidal or tabular (Russo and Punzo, 2004). Despite vesuvianite is a representative mineral of the Somma-Vesuvius volcanic complex, much sought by mineral collectors over time, to the authors' knowledge few detailed crystal-chemical and IR spectroscopy studies have been carried out to fully determine the nature of the vesuvianite species. In fact, vesuvian vesuvianite is generally treated in the frame of geochemical to petrological studies related to this volcanic complex.

This paper is addressed to a first characterization of a suite of twelve well-crystallized vesuvianites from Somma-Vesuvius ejecta by a combination of chemical, X-ray diffraction and FTIR single-crystal spectroscopic investigations, thus to provide better understanding of minerogenetic and petrologic processes and fluid evolution at magma chamber walls. The samples, some of them really spectacular, come from a private collection owned to Enrico Franco, professor of mineralogy

at Naples university, to whose memory this work is dedicated.

Brief outline on crystal chemical, structural and infrared studies of vesuvianite

From the structure refinement of Warren and Modell (1931) and for the subsequent fifty years, the definition of the chemical formula of vesuvianite was quite problematic. Then, Hoisch (1985) and Valley et al. (1985) established that a common end-member of the vesuvianite group could have the formula $Ca_{19}Mg_2Al_{11}Si_{18}O_{68}(OH, F)_9$. The vesuvianite structure displays alternating column-shaped subunits analogic with the structure of grossular; it has been considered both as an orthosilicate (Deer et al., 1997) and as a sorosilicate with mixed SiO_4 and Si_2O_7 groups (Strunz and Nickel, 2001) or ortho-diortho silicate (i.e. Paluszkiewicz and Zabinski, 1995; Galuskin et al., 2007a,b). Taking into account the isostructural varieties, the ideal formula of vesuvianite-group minerals can be represented as $X_{18}X'Y_{12}Y'T_5{}^OZ_{10}{}^DZ_8O_{68}(W)_{11}$ (Gnos and Armbruster, 2006; Elmi et al., 2011), where the site occupancies are:

X and X' sites - Ca (REE, U, Th, Pb, Bi, Pb, Sb, K, Ba, Sr, □), with [7]-, [8]-, and [9]-fold coordination;

Y and Y' sites - Al, Mg, Fe^{3+}, Fe^{2+}, Mn^{2+}, Mn^{3+},Ti (Zn, Cr, Cu^{2+}), with [6]- and [5]-fold coordination, respectively;

T sites - □, B (Al, Fe^{3+}, Mn^{3+}, Mg), with [4]- and [3]- coordination;

Z sites - Si, H_4, with [4]-fold coordination; 'O' and 'D' superscripts stand for orthosilicate and disilicate groups, respectively;

W site - OH, F, O (Cl).

In the vesuvianite group, wiluite contains B > 2.5 atoms per formula unit (apfu) at the T site, manganvesuvianite Mn^{3+} > 0.5 apfu at the Y' site and fluorvesuvianite F > 4.5 apfu at the W site. Chlorine does not usually exceed 0.05 apfu at the W site in low-temperature vesuvianites from rodingites, whereas it can vary between 0.1 and 0.8 apfu in high-temperature and fluorine-bearing vesuvianite from skarns (Galuskin et al., 2005).

As reported by Elmi et al. (2011 and reference therein) and Groat et al. (1996), many chemical substitutions are possible in vesuvianite, like:

$3(Mg^{2+}, Fe^{2+},Mn^{2+}) \leftrightarrow 2(Al^{3+}, Fe^{3+}) + \square$;
$2(Mg^{2+}, Fe^{2+},Mn^{2+}) \leftrightarrow Ti^{4+} + \square$;
$B^{3+} + Mg^{2+} + 2O^{2-} \leftrightarrow 2H^+ + Al^{3+} + 2OH^-$;
$(SiO_4)^{4-} \leftrightarrow (H_4O_4)^{4-}$;
$Ca + Al \leftrightarrow Na + Ti$;
$B^{3+} + 2O^{2-} \leftrightarrow \square + OH^-$.
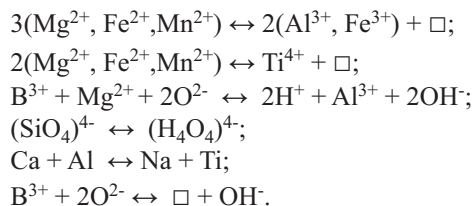
In accordance with some cases of anomalous optical behaviour, vesuvianite has been described, besides $P4/nnc$, in a number of other space groups, either tetragonal ($P4/n$, $P4nc$, P-4) or monoclinic ($P2/n$, Pn) (Arem and Burnham, 1969; Rucklidge et al., 1975; Giuseppetti and Mazzi, 1983; Fitzgerald et al., 1986; Groat et al., 1993; Ohkawa et al., 1994; Groat et al., 1994a; b, 1996; Pavese et al., 1998; Tribaudino and Prencipe, 1999; 2001; Armbruster and Gnos, 2000 a; b; c; Britvin et al., 2003; Galuskin et al., 2003a; b; 2007a; Ohkawa et al., 2009). The deviation from the $P4/nnc$ symmetry is related to X' and Y' site ordering and to channel-like rods in the structure oriented parallel to the c axis (Angel, 1986; Armbruster and Gnos, 2000b). Owing to the very short distance between two adjacent X' and Y' sites, a vacancy is necessarily introduced. Then, a rod is made either by Y'□X'□ or by □X'□Y' sequences, with a resultant polar arrangement of X' and Y'. In the $P4/nnc$ symmetry the adjacent rods are long-range disordered (random polarity), whereas in the lower symmetries (e.g. centro-symmetric $P4/n$ or acentric $P4nc$) they show precise ordering schemes. Many vesuvianite structures can be described in terms of mixed rod polytype or domain formation of

different rod polytypes. Single-crystal X-ray investigations cannot point out random rod orientation domains (*P4/nnc*) intercalated with ordered rod domains (*P4/n* or *P4nc*), due to the lack of distinctive diffraction features of the disordered rods. Moreover, rod polytypism cannot be studied by conventional powder X-ray diffraction, the additional *P4nc* and *P4/n* typical reflections being too weak to be detected (Gnos and Armbruster, 2006).

The temperature of formation of vesuvianite can be estimated by the cation arrangement at partially occupied Y' and X' sites; late-stage hydrothermal/metasomatic "low vesuvianites" thus show mainly a *P4/n* symmetry and form at T<300°C, whereas contact/regional metamorphic "high vesuvianites" normally show a *P4/nnc* symmetry and are related to T>500°C (Allen and Burnam, 1992).

The first infrared studies on vesuvianite were accomplished by Coda et al. (1970), Zabinski (1971) and Morandi et al. (1979). Then, polarized OH absorption spectra of vesuvianites from different localities and geologic environments were extensively studied by Groat et al. (1995) and by Paluszkiewicz and Zabinski (1995; 1999) and Lager et al. (1999) as well. A detailed study of the OH content of vesuvianites from volcanic ejecta from Latium (central Italy) was presented by Bellatreccia et al. (2005b; 2006), while polarized FTIR data of the boron absorption region were presented by Bellatreccia et al. (2005a). In general, the polarized OH spectra show great variability. Eight bands in the 3670-3380 cm^{-1} region are described which are caused by OH groups at the structural OH site with different local cation and anion configurations; four bands observed in the low-energetic 3250-3050 cm^{-1} range are attributed to OH groups, partially replacing the O(10) oxygen sites (Bellatreccia et al., 2005b). In boron-rich vesuvianites the latter four bands are not present. The high-energy group of bands is associated with a bent O(OH)-H(1)…O(7) hydrogen bond

system; evaluation of the band areas in both polarisation directions confirms an O-H vector orientation of ~ 35° tilted from the *c*-axis (Lager et al., 1999; Bellatreccia et al., 2005b). The low-energy group of bands is part of a straight O(10)-H(2)…O(10) bond system.

Studied samples

Ten samples of the batch considered for the present study come from vesuvianite-bearing skarn ejecta, while two vesuvianite specimens derive from a K-feldspar rich-, syenitic ejectum and from a composite rock showing sharp contacts between a prevailing syenite and skarn (Table 1). These ejecta can be associated with various plininan eruptive events, like the Avellino (ca. 3900-3700 yr. BP), Pompeii (A.D. 79) and Pollena (A.D. 472) eruptions (i.e. Rolandi et al., 2004; Di Renzo et al., 2007; Sevink et al., 2011). The vesuvianite crystals are dark brown to honey yellow-brown, rarely reddish-brown, and up to 2 centimetres in dimension. Figure 1 shows two typical occurrences of vesuvianite in the considered rocks.

Skarns display a variety of mineral assemblages and textures, sometimes with a composite nature leading to sharp transitions from skarn to marble or hornfels at hand specimen scale. Zoning and metasomatic fronts can be pointed out; clinopyroxene-phlogopite-wollastonite-calcite associations alternate with cavities rich in vesuvianite, calcic garnet, nepheline or anorthite. Other minor to trace minerals detected in these skarns in variable percentages can be leucite, olivine, clinohumite, cuspidine, Mg-Al-Fe spinel, fluorite, sodalite, meionite, davyne, gehlenite, magnetite, apatite, and REE-rich phases. Syenitic ejecta are igneous-looking and holocrystalline (medium to coarse-grained), with a leucocratic appearance mainly due to prevailing K-feldspar (sanidine) with accessory vesuvianite, clinopyroxene,

amphibole, garnet and sphene. In one sample, an abrupt change to a subordinate skarn-like, phlogopite + plagioclase + garnet + wollastonite-bearing part can be observed.

Methods

Single crystals of vesuvianites were easily separated from the rocks, due to both their large dimension and to the favorable position (geodes, external surfaces, etc.). Thus, many good-quality samples were available for analytical work. For each specimen, the dataset presented here refers to powders or fragments of the same crystal.

A preliminary check of the samples was made using powder X-ray measurements (XRPD) with a Seifert-GE MZVI diffractometer (Dipartimento di Scienze della Terra, Università di Napoli

Federico II), with $CuK\alpha$ radiation, Ni-filtred at 40 kV and 30 mA, 3-80 °2θ range, step scan 0.02°, time 10 sec/step. Powder diffraction patterns were processed using the RayfleX software package (GE).

X-ray diffraction experiments on samples SV1 to SV5 were carried out at room temperature by a Bruker-Nonius KappaCCD single crystal diffractometer, equipped with a charge-coupled device (CCD detector), using monochromatized MoK_α radiation (λ= 0.71073 Å). The automatic data collection strategy was defined by the COLLECT (Nonius, 2002) software, cell determination and refinement by DIRAX (Duisenberg, 1992) and data reduction by EVAL (Nonius, 2002). Absorption effects were corrected by SADABS (Sheldrick, 2002)

Table 1. Sample number, provenance site and main mineral phases associated with vesuvianite in the ejected rocks of Somma-Vesuvius considered in this study.

Sample no.	Locality	Ejectum type	Main mineral association
SV1	San Vito	skarn	clinopyroxene, phlogopite, garnet, leucite, wollastonite
SV2	San Sebastiano	skarn	clinopyroxene, phlogopite, wollastonite, meionite, olivine, spinel
SV3	San Vito	skarn	clinopyroxene, phlogopite, wollastonite, olivine, spinel, scapolite
SV4	Terzigno	syenite	feldspar, amphibole, garnet, sphene, zircon, sodalite
SV5	San Vito	skarn	clinopyroxene, phlogopite, wollastonite, calcite
SV6	San Vito	skarn	clinopyroxene, phlogopite, spinel, cuspidine, clinohumite, fluorite, gehlenite
SV7	Lagno di Pollena	skarn	clinopyroxene, phlogopite, anorthite, spinel
SV8	Terzigno	skarn	clinopyroxene, phlogopite, leucite, magnetite, apatite
SV9	San Vito	skarn	clinopyroxene, phlogopite, wollastonite, calcite, spinel
SV10	San Vito	skarn	clinopyroxene, phlogopite, wollastonite, anorthite, magnetite, spinel
SV11	Lagno di Pollena	skarn	clinopyroxene, phlogopite, leucite, spinel
SV12	San Vito	syenite/skarn	feldspar, mica, leucite, anorthite, clinopyroxene, wollastonite, garnet, sphene

Figure 1. Examples of Somma-Vesuvius ejecta with brownish crystals of vesuvianite (Ves). (a) no. SV1 and (b) no. SV12. Scale bar is 5 cm.

exploiting a semi-empirical approach. The space group was determined by SIR2011, the updated version of the package SIR2008 (Burla et al., 2007).

The unit cell edges of samples SV6 to SV12 were first evaluated using XRPD on at least 80 reflections, processed with UnitCell software (Holland and Redfern, 1997) and then checked by single-crystal X-ray investigations (Weissenberg camera STOE apparatus, Enraf-Nonius CAD4-F diffractometer, graphite monochromatized Cu$K\alpha$ radiation, room temperature, at Dipartimento di Chimica Università di Napoli "Federico II").

Mineral chemistry was determined with energy-dispersive spectrometry (EDS) at CISAG (University of Napoli "Federico" II, Italy) utilizing an Oxford Instruments Microanalysis Unit. The latter is equipped with an INCA X-act detector and a JEOL JSM-5310 microscope operating at 15 kV primary beam voltage, 50-100 mA filament current, variable spot size and 50 s net acquisition time. Measurements were done with an INCA X-stream pulse processor and the 4.08 version *Inca* software. The following reference standards were alternatively used: wollastonite (Si, Ca), corundum (Al), albite (Al, Si, Na), jadeite (Na), diopside (Mg), rutile (Ti), almandine (Fe), Cr_2O_3 or Cr pure metal (Cr), rhodonite (Mn), orthoclase (K), apatite (P), fluorite (F), barite (Ba), strontianite (Sr). No volatilization of F was observed during the point analyses. Analytical errors are 1% rel. for major elements and 3% rel. for minor elements.

Light elements (Li, Be, B) and other selected trace elements of vesuvianite specimens were determined by inductively-coupled plasma-mass spectrometry (ICP-MS) at Acme Analytical Laboratories Ltd. (Vancouver), using multiacid digestion or Na_2O_2 fusion techniques (minimum detection limits 0.01-1 ppm).

Fourier transform infrared (FTIR) measurements were performed on nine selected gem-quality crystals, providing high-quality material for experimental work. Under the optical microscope (actual total magnification of 400 x), the crystals proved in parts to be free from inclusions and impurities. Selected vesuvianite single-crystals were oriented by morphology and optical methods, then slabs polished parallel to the *c*-axis were prepared. Crystal samples thinned to 25 μm and in some cases to 20 μm were measured using a wire grid with a 500 x 500 μm mesh for support. Polarized single-crystal spectra were measured at room temperature conditions by means of the Bruker Hyperion 1000 microscope (LN$_2$ cooled MCT

detector) attached to the Bruker FTIR spectrometer Tensor 27 (Globar light source), equipped with a KRS-5 grid polariser. Spectra were averaged over 120 scans with a nominal resolution of 4 cm^{-1} using a measuring field of 100 x 100 µm. The spectra are displayed as linear absorption coefficients α in cm^{-1}. The linear absorption coefficient is defined as α = A/t, where A is the linear absorbance, $\log(I_0/I)$, and t is the thickness of the crystal slabs measured in cm. Band deconvolution into single Voigt-shaped absorption bands was provided by the program PeakFit (Jandel Scientific, 1995). The band position uncertainty is ± 2 cm^{-1}. Prior to the actual fitting procedure, significantly evolved interference fringes, distorting mainly the shape of the weaker bands in spectra measured perpendicular to the *c*-axis, had to be removed. This was accomplished by fitting a complex sine-function with six adjustable parameters (A_0-A_5) onto the 2050-2800 cm^{-1} and 3700-4500 cm^{-1} spectral regions, free of any vesuvianite OH absorptions:

$$Y = A_0 \cdot \sin\{[(X \cdot A_1) + A_2] \cdot 2\pi\} \cdot \sin\{[(X - A_3)/(A_4 + A_5) \cdot (X - X_{MIN})] \cdot 2\pi\}$$

The parameters A_0, A_1 and A_2 modulate the amplitude changes of the interference fringe; the other three parameters determine the actual sine oscillation caused by the interference. X_{MIN} is the minimum value of the X variable within the fitted spectral region. This function had to be superimposed on another primitive sine function, compensating for the general changes in the behaviour of the spectral curve in the fitted regions. By subtracting the Y values obtained using the fitted function (1) from the entire 2050-4500 cm^{-1} region, including the vesuvianite OH absorptions, the interference artifact was almost entirely removed. For the evaluation of the water content, the integrated absorbance values A_i (cm^{-1}) measured on sections cut parallel to the *c*-axis were summed up to get the total integrated

absorbance value $A_{i\ tot}$ ($A_{i\ tot} = 2\ A_{i\ perpend\ c} + A_{i\ parall\ c}$) which was used for the calculation of the integrated absorption coefficient α_i (cm^{-2}; $\alpha_i = A_{i\ tot}/t$). As expressed by Beer's law, α_i is directly related by the integrated molar absorption coefficient ε_i (l mol$^{-1}_{H2O}$ cm^{-2}) to the concentration c (mol l^{-1}). The water content in wt% is c_{H2O} = (1.8/D) (α_i/ε_i), where D is the density of the mineral (3.4 g cm^{-3} for vesuvianite). The ε_i value for OH in vesuvianite determined by Bellatreccia et al. (2005b) on the basis of SIMS data amounts to 100000 ± 2000 l mol$^{-1}_{H2O}$ cm^{-2}. The choice of the 'broken-line' background coincides with that proposed by these authors.

The amount of lattice OH of three samples were evaluated through thermo-gravimetric analyses (TGA) using a Thermoflex Rigaku thermal analyzer apparatus under flowing nitrogen (Dipartimento di Scienze Chimico-Agrarie, Naples), programmed to raise the temperature from 25° to1000 °C at a rate of 10 °C/min. Analytical error is 5 % rel. for the calculated water contents.

The identification of whole-rock mineral assemblages was accomplished by means of combined polarized optical microscopy, XRPD and qualitative-quantitative EDS microanalysis.

Results

Chemical composition and X-ray diffraction

The chemical composition of the studied vesuvianites is reported in Table 2, and was obtained by combining EDS (Si, Al, Ti, Mg, Mn, Fe, Ca, Na, K, Ba, Sr, F and Cl) and ICP-MS (B, Be Li, Y, REE, Th, U) data; OH$^-$ was mainly derived by FTIR single-crystal measurements, whereas for three samples the water content was evaluated by TGA. The crystal-chemical formulae were based on 18 Si atoms, assuming that the observed limited variations in Z-O bond lengths generally suggest full Si occupancy at Z sites (Groat et al., 1994b). The analysed vesuvianites have rather constant contents of

Table 2. Chemical composition (wt.%) of vesuvianite from Somma-Vesuvius volcanic complex, with their chemical formulae (apfu) normalized on 18 Si atoms (Groat et al., 1994).

Sample no.	SV1	SV2	SV3	SV4	SV5	SV6	SV7	SV8	SV9	SV10	SV11	SV12
n*	10	12	9	5	12	10	8	10	11	9	12	6
SiO_2	37.05	36.91	37.20	36.29	36.25	36.72	37.30	36.79	36.82	37.00	36.95	37.06
Al_2O_3	16.26	16.51	16.44	15.30	15.13	16.15	16.97	16.20	16.30	16.99	15.87	16.98
TiO_2	0.43	0.16	0.24	0.67	0.35	0.16	0.29	0.25	0.17	0.18	0.37	0.22
MgO	2.52	2.58	2.67	2.89	2.92	2.84	2.84	2.77	2.66	2.88	2.62	2.66
MnO	0.45	0.37	0.51	0.78	0.70	0.36	0.36	0.45	0.30	0.04	0.43	0.20
Fe_2O_3**	4.88	4.44	4.79	5.16	5.65	4.90	3.90	4.90	4.47	4.21	4.82	4.47
CaO	35.83	35.67	35.78	35.20	35.46	35.93	35.93	35.97	35.76	35.80	35.97	35.44
Na_2O	0.09	0.16	0.10	0.11	0.10	0.04	0.04	0.07	0.09	0.13	0.08	0.08
K_2O			0.01		0.02	0.02	0.02	0.02	0.01	0.02		
BaO		0.02	0.01	0.02				0.02	0.02	0.04	0.01	
SrO			0.02						0.04		0.02	0.03
B_2O_3	0.096	0.091	0.141	0.155	0.182	0.137	0.155	0.155	0.168	0.096	0.173	0.109
BeO	0.067	0.062	0.062	0.067	0.073	0.079	0.062	0.073	0.011	0.079	0.090	0.084
Li_2O	0.003	0.003	0.006	0.006	0.008	0.006	0.006	0.003	0.011	0.003	0.006	0.008
$S(REE,Y)_{ox}$	0.062	0.072	0.057	0.072	0.093	0.087	0.072	0.117	0.081	0.083	0.330	0.252
$S(Th,U)_{ox}$	0.026	0.017	0.030	0.023	0.061	0.052	0.023	0.022	0.023	0.021	0.024	0.009
F	1.77	1.44	1.56	2.25	1.77	1.62	1.61	1.65	1.41	1.62	1.55	1.52
Cl	0.01	0.01	0.02	0.02	0.04	0.04	0.04	0.05	0.01	0.02	0.02	0.02
H_2O***	1.003	0.915	0.771	0.725	0.671	0.891	0.767	0.775	0.968	0.663	1.007	1.025
	100.55	99.43	100.42	99.74	99.48	100.03	100.40	100.32	99.30	99.84	100.16	100.17
O=F,Cl	0.75	0.61	0.66	0.95	0.75	0.69	0.69	0.71	0.60	0.69	0.66	0.64
Total	99.80	98.82	99.76	98.79	98.73	99.34	99.71	99.61	98.70	99.15	99.50	99.53
Si	18.000	18.000	18.000	18.000	18.000	18.000	18.000	18.000	18.000	18.000	18.000	18.000
Al	9.301	9.478	9.365	8.53	8.304	8.966	9.644	8.924	9.380	9.477	9.102	9.705
Mg	1.573	1.682	1.595	1.966	2.160	2.019	1.688	1.994	1.789	1.899	1.818	1.499
Fe^{3+}	1.784	1.629	1.744	1.926	2.111	1.807	1.416	1.804	1.644	1.541	1.767	1.634
Ti	0.157	0.059	0.087	0.250	0.131	0.059	0.105	0.092	0.063	0.066	0.136	0.080
Mn	0.185	0.152	0.209	0.328	0.294	0.149	0.147	0.186	0.124	0.016	0.177	0.082
Sum Y	13.000	13.000	13.000	13.000	13.000	13.000	13.000	13.000	13.000	12.999	13.000	13.000
Ca	18.649	18.636	18.548	18.704	18.864	18.869	18.576	18.854	18.729	18.658	18.772	18.441
Mg	0.252	0.194	0.331	0.170	0.002	0.057	0.356	0.027	0.150	0.189	0.085	0.427
Na	0.085	0.151	0.094	0.106	0.096	0.038	0.037	0.066	0.085	0.123	0.076	0.075
K			0.006		0.013	0.013	0.012	0.012	0.006	0.011		
Ba		0.004	0.002	0.004				0.004	0.004	0.008	0.002	
Sr			0.006						0.011		0.006	0.008
$S(REE,Y)_{ox}$	0.001	0.013	0.010	0.013	0.019	0.018	0.013	0.023	0.020	0.015	0.059	0.047
$S(Th,U)_{ox}$	0.013	0.002	0.003	0.003	0.007	0.006	0.003	0.002	0.003	0.002	0.002	0.001
Sum X	19.000	19.000	19.000	19.000	19.001	19.001	19.001	18.999	19.001	19.000	19.000	18.999
B	0.081	0.077	0.118	0.133	0.157	0.117	0.130	0.132	0.143	0.081	0.146	0.092
Be	0.078	0.073	0.072	0.080	0.087	0.093	0.072	0.086	0.013	0.092	0.105	0.098
Li	0.006	0.006	0.012	0.012	0.016	0.012	0.012	0.006	0.022	0.006	0.012	0.016
Al	0.009	0.011	0.010	0.414	0.549	0.364	0.007	0.417	0.011	0.264	0.009	0.014
vacancy	4.826	4.833	4.788	4.361	4.191	4.414	4.779	4.359	4.811	4.557	4.728	4.780
Sum T	5.000	5.000	5.000	5.000	5.000	5.000	5.000	5.000	5.000	5.000	5.000	5.000
F	2.719	2.221	2.387	3.529	2.779	2.511	2.457	2.553	2.180	2.492	2.388	2.334
Cl	0.010	0.008	0.016	0.017	0.034	0.033	0.033	0.041	0.008	0.016	0.017	0.016
OH	3.25	2.976	2.488	2.399	2.222	2.913	2.469	2.529	3.156	2.151	3.272	3.321
O	4.021	4.795	5.109	4.055	4.965	4.543	5.041	4.877	4.656	5.341	4.879	4.329
Sum W	10.000	10.000	10.000	10.000	10.000	10.000	10.000	10.000	10.000	10.000	10.000	10.000

* No. of point analyses.   ** Total Fe calculated as Fe_2O_3.   Water content derived from both FTIR (SV1, SV2, SV3, SV4, SV5, SV7, SV9, SV10, SV11) and from thermo-gravimetric analyses (SV6, SV8, SV12).

major elements (i.e. 36.29 - 37.30 wt. % SiO_2, 15.13 - 16.99 wt. % Al_2O_3 and 35.20 - 35.80 wt.% CaO) and MgO (2.52 - 2.92 wt. %), with slightly more variable Fe_2O_3 amounts (3.90 - 5.95 wt. %). MnO varies between 0.04 and 0.78 wt. % and TiO_2 contents range from 0.16 wt. % to 0.43 wt. %. In all samples, light elements (B, Be and Li), Y, REE and actinides (Th, U) have been detected, with ranges of 0.09 - 0.18 wt. % B_2O_3, 0.01-0.09 wt. % BeO and 0.003-0.011 wt.% Li_2O. The REE content is low, with $\Sigma(Ree,Y)_{ox}$ up to 0.33 wt. %. Minor constituents are actinides [$\Sigma(Th,U)_{ox}$ up to 0.05 wt. %]. Na, K, Sr and Ba were also detected in small to negligible amounts. Additional trace and ultratrace elements were detected by ICP-MS analyses in some samples, with percentages between 200 and 40 ppm of V, Zn, Zr, Sn and <

15 ppm of Co, Ga, Nb, Ta, Hf, Pb, Bi. Regarding the volatiles, the studied vesuvianites are all characterized by quite high amounts of fluorine, ranging between 1.41 and 2.25 wt. % F; the water content is in the range 0.67 -1.03 wt. % H_2O, whereas chlorine is always observed in trace contents (0.01 - 0.05 wt. % Cl).

By comparison with other samples from Somma-Vesuvius volcanic complex, the studied vesuvianites show a quite pronounced variation in Mn and an enrichment in Fe and F+Cl (Figure 2). No evidence of significant chemical zoning or alteration has been found in the investigated crystals.

Single-crystal X-ray diffraction analyses of vesuvianite indicate that the crystals are tetragonal with cell parameters varying from
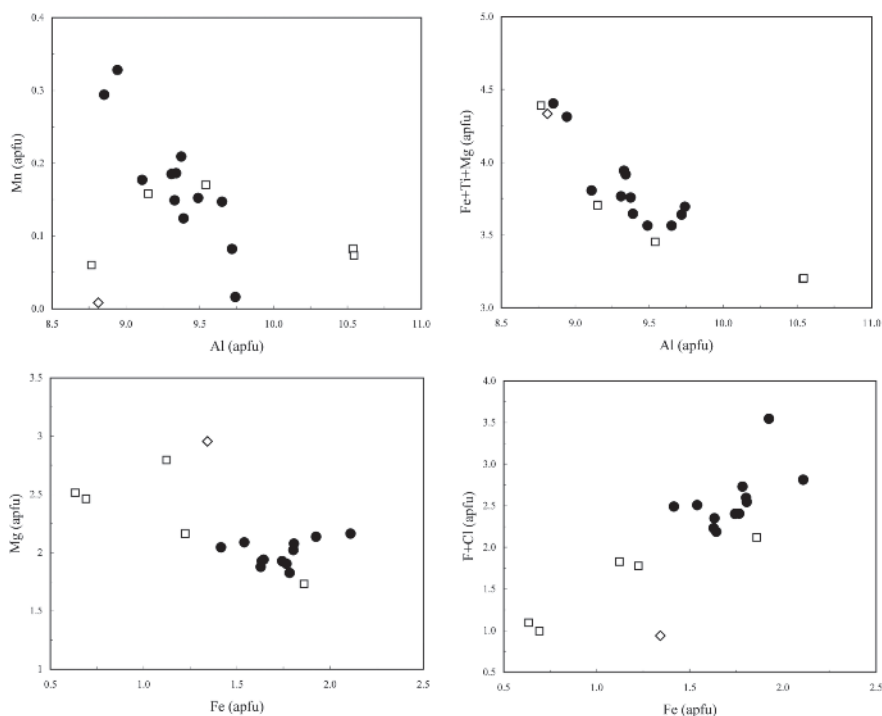
Figure 2. Composition diagrams for selected major and minor elements of vesuvianites from Somma-Vesuvius. Filled circles - vesuvianite from this study; empty squares - vesuvianite from Gilg et al. (2001); empty diamond - sample from Elmi et al. (2011).

15.542 Å up to 15.576 Å for *a* and from 11.800 Å up to 11.827 Å for *c*, as shown in Table 3. For samples SV1 to SV5, measured using the CCD single-crystal apparatus, the structure factor moduli, suitably corrected by absorption effects, were processed by SIR2011 package that was able to recognize *P*4/*nnc* as the most probable space group, in agreement with the already published investigations of skarn-derived, high-temperature vesuvianite from Somma-Vesuvius (Elmi et al., 2011). The same space group has also been deduced from measurements made by conventional Weissenberg mode. When plotted in the *c* vs *a* diagram, the studied crystals fall in a fairly restricted area that overlaps with the B-free vesuvianite, the hydrovesuvianite, the Mn-bearing vesuvianite and the *P*4/*ncc* vesuvianite areas (Figure 3).

Single-crystal polarized FTIR study

Polarized IR absorption spectra in the OH fundamental vibrational region (4000-2500 cm^{-1}) of selected vesuvianite crystals were measured parallel and perpendicular to the *c*-axis and are shown in Figure 4. The polarized spectra of the OH fundamental measured parallel to the *c*-axis are dominated by absorption bands at 3638, 3567, 3452 and 3200 cm^{-1}. As shown in Figure 5, spectral deconvolution reveals two additional bands centred at 3590 and 3117 cm^{-1}. All bands show strong pleochroism with maximum absorption parallel to the *c*-axis and weak absorption components perpendicular to *c*. However, the spectra measured perpendicular to the *c*-axis are also dominated by the 3567, 3590 and 3638 cm^{-1} band group, which are significantly weaker than parallel to the *c*-axis. Although the spectra of all the samples are very similar and display the same absorption bands in some samples, the 3638 cm^{-1} band is much less pronounced. Furthermore, the overall amplitude ratio between the 3567 and 3590 cm^{-1} doublet band and the lower-energetic bands varies between about 2:1 to 3:1. Water contents have been calculated using the total integrated absorption coefficient derived from the fitted spectra. The contents are consistent within each of the samples and range from 0.66 to 1.00 wt. % (Table 4). The water contents of 0.78, 0.89 and 1.03 wt. % obtained by TGA for samples SV6, SV8 and SV12, respectively, are in good agreement with the FTIR data. As mentioned before, according to Groat et al. (1992a, 1994b) an exchange vector $B^{3+} + Mg^{2+} + 2O^{2-} \leftrightarrow 2H^+ +$

Table 3. Sample numbers, unit cell data and crystal sizes of vesuvianites for XRD study.

Sample no.	Cell parameters (Å)		Cell volume (Å^3)	Crystal size (mm)
	a	*c*		
SV1	15.559(2)	11.812(3)	2859.3(9)	0.10 x 0.250 x 0.35
SV2	15.557(2)	11.800(2)	2855.9(7)	0.150 x 0.200 x 0.225
SV3	15.574(3)	11.805(2)	2863.3(9)	0.075 x 0.175 x 0.250
SV4	15.542(2)	11.801(1)	2850.8(7)	0.125 x 0.175 x 0.250
SV5	15.554(2)	11.803(3)	2855.3(9)	0.175 x 0.20 x 0.25
SV6	15.569(3)	11.814(3)	2863.6(3)	0.28 x 0.30 x 0.30
SV7	15.565(1)	11.815(2)	2863.1(3)	0.20 x 0.37 x 0.39
SV8	15.567(4)	11.818(4)	2863.9(7)	0.27 x 0.34 x 0.34
SV9	15.568(2)	11.821(3)	2864.9(6)	0.20 x 0.24 x 0.25
SV10	15.576(3)	11.825(4)	2868.9(6)	0.26 x 0.26 x 0.29
SV11	15.561(2)	11.822(3)	2862.6(4)	0.29 x 0.29 x 0.32
SV12	15.568(3)	11.827(4)	2866.4(2)	0.23 x 0.28 x 0.35
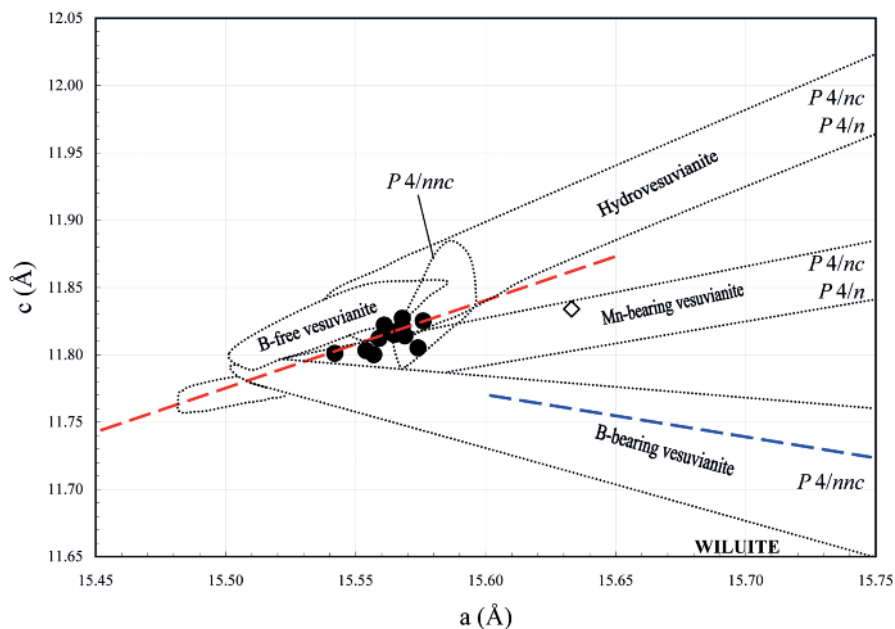
Figure 3. Plot of the studied vesuvianite cell dimensions (filled circles), with the indication of the main substitution trends (areas bordered by dotted lines areas) and the space groups according to Gnos and Armbruster (2006). The empty diamond is the sample from Elmi et al. (2011), whereas the red and blue dashed lines are approximate trends (not least-square data fits) of boron-free and boron-bearing vesuvianites, respectively, as reported by Groat et al. (1992a).

Al^{3+} + $2OH^-$ can be inferred in B-bearing vesuviantes, resulting in an inverse correlation between OH and Mg. This behaviour has also been recorded by Bellatreccia et al. (2005a, 2005b) in B-rich vesuvianites from Latium. Despite the Somma-Vesuvius vesuvianite studied here contains low - but constantly present - amounts of boron, when plotted in the OH vs Mg diagram a linear trend and a negative correlation, recorded for B-rich varieties, is also obtained (Figure 6), in accordance with the above mentioned substitution mechanism.

Concluding remarks

Preliminary investigations on vesuvianite from skarn and syenitic ejecta of Vesuvius have shown a mainly fluorine-rich composition, and a constant occurrence of other volatiles like OH and chlorine. Other peculiar features are the constant presence of light elements (B, Be, Li), of REE and Y and of the actinides Th and U; many other trace and ultratrace elements (Zr, V, Zn, Sn, Co, Ga, Nb, Ta, Hf, Pb, Bi) are always detected. The space group, identified as *P4/nnc*, is consistent with the high-temperature crystallization conditions, as also evidenced by the nature of the host rocks and the associated mineral assemblages.

A detailed estimate of the formation temperature and chemical environment of skarn minerals at Somma-Vesuvius was established by Gilg et al. (2001) through fluid inclusion studies. According to these authors, vesuvianite contains only saline melt and/or silicate-free multiphase aqueous brine inclusions, trapped at temperatures
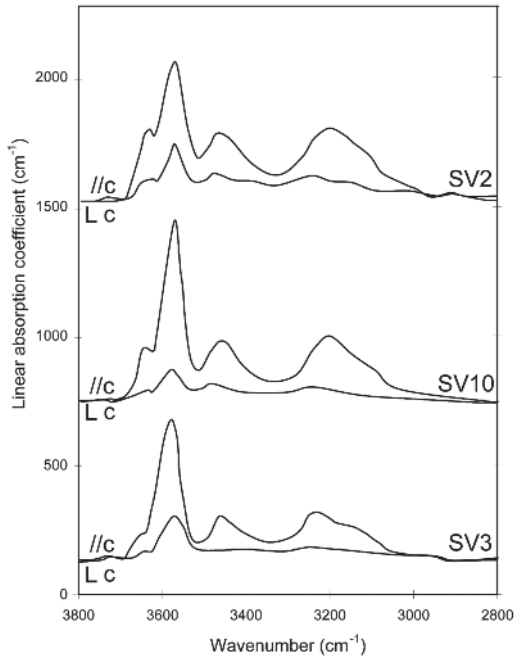
Figure 4. Polarized IR absorption spectra in the OH stretching vibrational range of selected vesuvianite crystals, measured parallel and perpendicular to the *c*-axis.
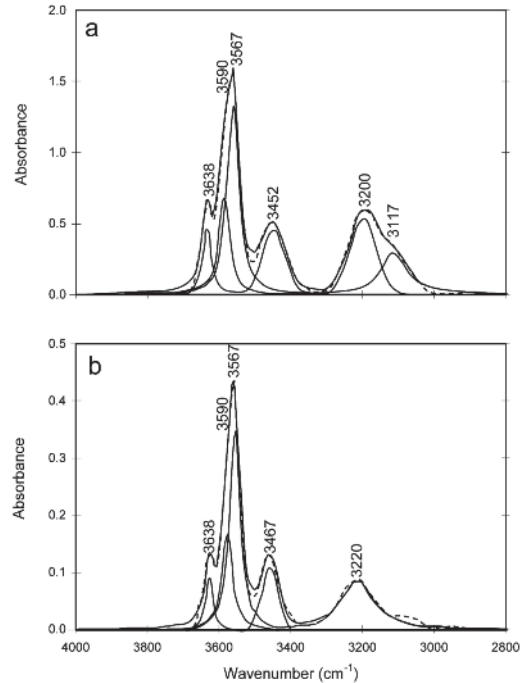
Figure 5. Polarized OH absorption spectra of vesuvianite (sample SV9) measured (a) parallel and (b) perpendicular to the *c*-axis. Spectra are baseline-corrected and decomposed into single Voigt-shaped absorption bands. Note the different absorbance scale.

Table 4. FTIR data of vesuvianite samples: the calculated water content (analytical error is 4% rel.), the total integrated absorbance values Ai and the thickness of the measured crystal slabs (see text).

Sample no.	H_2O (wt. %)	$A_i//c$ (cm^{-1})	$A_i \perp c$ (cm^{-1})	Thickness (μm)
SV1	1.003	335.515	49.948	23
SV2	0.915	246.776	66.591	22
SV3	0.771	178.230	41.906	18
SV4	0.725	220.080	67.896	26
SV5	0.671	166.502	62.412	23
SV7	0.767	323.944	84.217	34
SV9	0.968	292.060	55.053	22
SV10	0.663	230.223	35.277	24
SV11	1.007	246.876	38.186	17
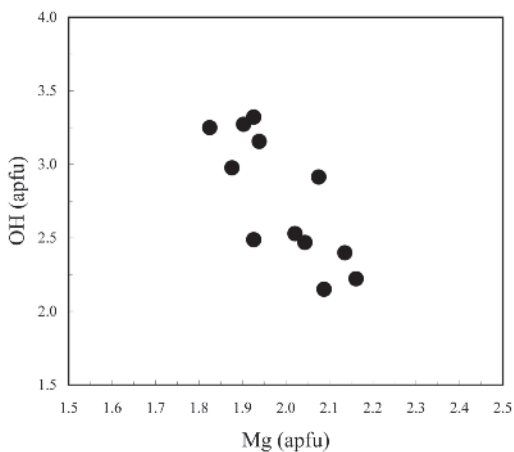
Figure 6. Relationship between the OH amounts versus Mg for the studied vesuvianite.

of at least 800-890 °C. They found neither evidence of fluid circulation below 700 °C, nor of a convectively cooling hydrothermal system or involvement of externally derived meteoric fluids in skarn formation at the magma-carbonate wall rock interface, thus confirming the high-temperature genesis of vesuvianite. Fluid and melt inclusions also show that the Vesuvian skarn formation is mostly related to chloride-fluoride-sulfate-carbonate-rich saline fluids, that were also important in transporting significant amounts of incompatible elements from the magma into the wall rocks. This is also confirmed by the presence of REE, Ti, Y, Th, U, Zr always detected in our vesuvianite, as well as of accessory minerals containing these elements in the investigated rocks. The significant amounts of fluorine partitioned into the saline aqueous fluid phase involved in the metasomatic process is demonstrated by the overall F-rich nature of the vesuvianites studied, but also by the occurrence of mineral phases like for example phlogopite and clinohumite in the skarn assemblages. High temperatures ($\geq$ 800 °C) and metasomatic, volatile-rich (H_2O, F, CO_2, Cl and S) fluids of

magmatic origin are also compatible with the genesis of vesuvianite in its K-feldspar-rich hosts.

Work is still in progress on Somma-Vesuvius vesuvianites, in order to better clarify various aspects of their crystal chemistry, by means of both structure refinement of phases from different hosts and Mössbauer spectroscopy to establish the valence state of iron.

Acknowledgments

References

Angel R.J. (1986) - Polytypes and polytypism. *Zeitschrift für Kristallographie*, 176, 193-204.

Allen F.M. and Burnham C.W. (1992) - A comprehensive structure-model for vesuvianite: symmetry variation and crystal growth. *Canadian Mineralogist*, 30, 1-18.

Arem J.E. and Burnham C.W. (1969) - Structural variations in idocrase. *American Mineralogist*, 54, 1546-1550.

Armbruster T. and Gnos E. (2000a) - Tetrahedral vacancies and cation ordering in low-temperature Mn-bearing vesuvianites: Indication of a hydrogarnet-like substitution. *American Mineralogist*, 85(3-4), 570-577.

Armbruster T. and Gnos E. (2000b) - *P*4/*n* and *P*4*nc* long-range ordering in low-temperature

vesuvianites. *American Mineralogist*, 85, 563-569

Armbruster T. and Gnos E. (2000c) - ''Rod'' polytypism in vesuvianite: crystal structure of a low-temperature *P4nc* vesuvianite with pronounced octahedral cation ordering. *Schweizer Mineralogische und Petrographische Mitteilungen,* 80, 109-116.

Armbruster T., Gnos E., Dixon R., Gutzmer J., Hejny C., Döbelin N. and Medenbach O. (2002) - Manganvesuvianite and Tweddillite, two new Mn^{3+}-silicate minerals from the Kalahari Manganese fields, South Africa. *Mineralogical Magazine*, 66, 137-150.

Bellatreccia F., Della Ventura G., Williams C.T., Lumpkin G.R., Smith K.L. and Colella M. (2002) - Non-metamict zirconolite polytypes from the feldspathoid-bearing alkali-syenitic ejecta off the Vico volcanic complex (Latium, Italy). *European Journal of Mineralogy,* 14, 809-820.

Bellatreccia F., Cámara F., Ottolini L., Della Ventura G., Cibin G. and Mottana A. (2005a) - Wiluite from Ariccia, Latium (Italy): occurrence and crystal structure. *Canadian Mineralogist*, 43, 1457-1468.

Bellatreccia F., Della Ventura G., Ottolini L., Libowitzky E. and Beran A. (2005b) - The quantitative analysis of OH in vesuvianite: a polarized FTIR and SIMS study. *Physics and Chemistry of Minerals,* 32, 65-76.

Bellatreccia F., Ottolini L. and Della Ventura G. (2006) - Microanalysis of H and B in vesuvianite by SIMS, EMPA and FTIR. *Microchimica Acta*, 155, 91-94.

Britvin S.N., Antonov A.A., Krivovichev S.V., Armbruster T., Burns P.C. and Chukanov N.V. (2003) - Fluorvesuvianite, $Ca_{19}(Al,Mg,Fe^{2+})_{13}$ $[SiO_4]_{10}[Si_2O_7]_4O(F,OH)_9$, a new mineral species from Pitkäranta, Karelia, Russia: Description and crystal structure. *Canadian Mineralogist*, 41, 1371-1380.

Burla M.C., Caliandro R., Camalli M., Carrozzini B., Cascarano G.L., De Caro L., Giacovazzo C., Polidori G., Siliqi D. and Spagna R. (2007) - IL MILIONE: a suite of computer programs for crystal structure solution of proteins. *Journal of Applied Crystallography,* 40, 609-613.

Ciriotti M.E., Fascio L. and Pasero M. (2009) - Italian type minerals. Ed. Plus, Pisa University Press, 357 pp.

Coda A., Della Giusta A., Isetti G. and Mazzi F. (1970) - On the structure of vesuvianite. *Atti dell'Accademica delle Scienze di Torino,* 105, 1-22.

Deer W.A., Howie R.A. and Zussman M.A. (1997) - Rock-forming minerals. Orthosilicate. Volume 1A. The Geological Society, London, 919 pp.

Della Ventura G., Mottana A., Parodi G.C., Raudsepp M., Bellatreccia F., Caprilli E., Rossi P. and Fiori S. (1996) - Monazite-huttonite solid-solutions from the Vico Volcanic Complex, Latium, Italy. *Mineralogical Magazine*, 60, 751-758.

Della Ventura G., Williams T.C., Cabella R., Oberti R., Caprilli E. and Bellatreccia F. (1999) - Britholite - hellandite intergrowths and associated REE-minerals from the alkali-syenitic ejecta of the Vico volcanic complex (Latium, Italy): petrological implications bearing on REE mobility in volcanic systems. *European Journal of Mineralogy*, 11, 843-854.

Di Renzo V., Di Vito M.A., Arienzo I., Carandente A., Civetta L., D'Antonio M., Giordano F., Orsi G. and Tonarini F. (2007) - Magmatic history of Somma-Vesuvius on the basis of new geochemical and isotopic data from a deep borehole (Camaldoli della Torre). *Journal of Petrology,* 48-4, 753-784.

Duisenberg A.J.M. (1992) - Indexing in single-crystal diffractometry with an obstinate list of reflections. *Journal of Applied Crystallography,* 25, 92-96.

Elmi C., Brigatti M.F., Pasquali L., Montecchi M., Laurora A., Malferrari D. and Nannarone S. (2011) - High-temperature vesuvianite: crystal chemistry and surface considerations. *Physics and Chemistry of Minerals*, 38-6, 459-468.

Fitzgerald S.F., Rheingold A.R. and Leavens P.B. (1986) - Crystal structure of a non-*P4/nnc* vesuvianite from Asbestos, Quebec. *American Mineralogist*, 71,1483-1488.

Galuskin E.V., Armbruster V., Malsy A., Galuskina I.O. and Sitarz M. (2003a) - Morphology, composition and structure of low-temperature *P4/nnc* high-fluorine vesuvianite from Polar Yakutia, Russia. *Canadian Mineralogist*, 41-4, 843-856.

Galuskin E.V., Galuskina I.O., Sitarz M. and Stadnicka K. (2003b) - Si-deficient, OH-substituted, boron-bearing vesuvianite from the Wiluy River, Yakutia, Russia. *Canadian Mineralogist* , 41, 833-842.

Galuskin E.V., Galuskina I. and Dzierżanowski P. (2005) - Chlorine in vesuvianites. *Mineralogia Polonica,* 36, 51-61.

Galuskin E.V., Galuskina I.O., Stadnicka K.,

Armbruster T. and Kozanecki M. (2007a) - The crystal structure of Si-deficient, OH-substituted, boron-bearing vesuvianite from the Wiluy River, Sakha-Yakutia, Russia. *Canadian Mineralogist,* 45(2), 239-248.

Galuskin E.V., Janeczek J., Kozanecki M., Sitarz M., Jastrzębski W., Wrzalik R. and Stadnicka K. (2007b) - Single-crystal Raman investigation of vesuvianite in the OH region. *Vibrational spectroscopy*, 44, 36-41.

Gilg A.H., Lima A., Somma R., Belkin H.E., De Vivo B. and Ayuso R.A. (2001) - Isotope geochemistry and fluid inclusion study of skarns from Vesuvius. *Mineralogy and Petrology*, 73, 145-176.

Giuseppetti G. and Mazzi F. (1983) - The crystal structure of a vesuvianite with $P4/n$ symmetry. *Tschermaks Mineralogische und Petrographische Mitteilungen*, 31, 277-288.

Gnos E. and Armbruster T. (2006) - Relationship among metamorphic grade, vesuvianite "rod polytypism," and vesuvianite composition. *American Mineralogist,* 91/5-6, 862 - 870.

Groat L.A., Hawthorne F.C. and Ercit T.S. (1992a) - The chemistry of vesuvianite. *Canadian Mineralogist*, 30, 19-48.

Groat L.A., Hawthorne F.C. and Ercit T.S. (1992b) - The role of fluorine in vesuvianite: a crystal-structure study. *Canadian Mineralogist*, 30, 1065-1075.

Groat L.A., Hawthorne F.C., Ercit T.S. and Putnis A. (1993) - The symmetry of vesuvianite. *Canadian Mineralogist,* 31, 617-635.

Groat L.A., Hawthorne F.C. and Ercit T.S. (1994a) - Excess Y-group cations in the crystal structure of vesuvianite. *Canadian Mineralogist,* 32, 497-504.

Groat L.A., Hawthorne F.C. and Ercit T.S. (1994b) - The incorporation of boron into the vesuvianite structure. *Canadian Mineralogist,* 32, 505-523.

Groat L.A., Hawthorne F.C., Rossman G.R. and Ercit T.S. (1995) - The infrared spectroscopy of vesuvianite in the OH region. *Canadian Mineralogist,* 33, 609-626.

Groat L.A., Hawthorne F.C., Lager G.A., Schultz A.J. and Ercit T.S. (1996) - X-ray and neutron crystal-structure refinements of a boron bearing vesuvianite. *Canadian Mineralogist,* 34, 1059-1070.

Groat L.A., Hawthorne F.C., Ercit T.S. and Grice J.D. (1998) - Wiluite, $Ca_{19}(Al,Mg,Fe,Ti)_{13}(B,Al,)_5$ $Si_{18}O_{68}(O,OH)_{10}$, a new mineral isostructural with vesuvianite, from Sakha Republic, Russian Federation. *Canadian Mineralogist,* 36, 1301-1304.

Hoisch T.D. (1985) - The solid solution chemistry of vesuvianite. *Contributions to Mineralogy and Petrology,* 89, 205-214.

Holland T.J.B. and Redfern S.A.T. (1997) - Unit cell refinement from Powder diffraction data: the use of regression diagnostics. *Mineralogical Magazine*, 61, 65-77.

Jandel Scientific (1995) - PeakFit - Peak separation and analysis software for Windows. San Rafael CA, USA.

Kappeler M.A. (1723) - Prodromus Crystallographiae de Crystallis Improprie sic dictis Commentarium. Heinrich Rennward Wyssing, Ed. Lucerna, Switzerland, 43 pp.

Lager G.A., Xie Q., Ross F.K., Rossman G.R., Armbruster T., Rotella F.J. and Schultz A.J. (1999) - Hydrogen-atom positions in $P4/nnc$ vesuvianite. *Canadian Mineralogist*, 37, 763-768.

Libowitzky E. and Beran A. (2004) - IR spectroscopic characterisation of hydrous species in minerals. In: Beran A., Libowitzky E. (eds) Spectroscopic methods in mineralogy. EMU Notes in Mineralogy, 6, 227-279.

Morandi N., Minguzzi V. and Nannetti M.C. (1979) - Spettri IR, comportamento termico e prodotti di riscaldamento di vesuviane e granati variamente idrati. *Mineralogica e Petrografica Acta,* 23, 151-173.

Nonius (2002) - COLLECT and EVAL. Nonius BV, Delft, The Netherlands.

Nyunt T.T., Theye T. and Massonne H.J. (2009) - Na-rich vesuvianite in jadeitite of the Tawmaw jade district, Northern Myanmar. *Periodico di Mineralogia*, 78, 5-18.

Ohkawa M., Yoshiasa A. and Takeno S. (1994) - Structural investigation of high and low-symmetry vesuvianite. *Mineralogical Journal*, 17, 1-20.

Ohkawa M., Armbruster T. and Galuskin E. (2009) - Structural investigationof low-symmetry vesuvianite collected from Tojyo, Hiroshima, Japan: implications for hydrogarnet-like substitution. *Journal of Mineralogical and Petrological Sciences,* 104-2, 69-76.

Paluszkiewicz C. and Zabinski W. (1995) - H bonding in vesuvianite, a complex ortho-disilicate. *Vibrational Spectroscopy*, 8, 315-318.

Paluszkiewicz C. and Zabinski W. (1999) - NIR spectra in vesuvianite - a complex ortho-disilicate mineral. *Journal of Molecular Structure*, 480-481, 683-688.

Pavese A., Prencipe M., Tribaudino M. and Aagaard S.S. (1998) - X-ray and neutron single crystal study of *P*4/*n* vesuvianite. *Canadian Mineralogist*, 36,1029-1037.

Rolandi G., Munno R. and Postiglione A. (2004) - The 427 A.D. eruption of Somma volcano. *Journal of Volcanology and Geothermal Research*, 129-4, 291-319.

Rucklidge J.C., Hemingway B.S. and Fisher J.R. (1975) - The crystal structure of three Canadian vesuvianites. *Canadian Mineralogist*, 13, 15-21.

Russo M. and Punzo I. (2004) - I minerali del Somma-Vesuvio. AMI, Cremona, 320 pp.

Sevink J., van Bergen M.J., van der Plicht J., Feiken H., Anastasia C. and Huizinga A. (2011) - Robust date for the Bronze Age Avellino eruption (Somma-Vesuvius): 3945 ± 10 calBP (1995 ± 10 calBC). *Quaternary Science Review*, 30, 1035-1046.

Sheldrick G.M. (2002) - SADABS. Version 2.03. University of Göttingen, Germany.

Strunz H. and Nickel E.H. (2001) - Strunz Mineralogical Tables. E. Schweizerbarth'sche Verlagsbuchhandlung, Nägele u. Obermiller, Stuttgart, 870 pp.

Tribaudino M. and Prencipe M. (1999) - A high temperature in situ single crystal study of *P*4/*n* vesuvianite. *European Journal of Mineralogy*, 11, 1037-1042.

Tribaudino M. and Prencipe M. (2001) - The compressional behaviour of the *P*4/*n* vesuvianite. *Canadian Mineralogist*, 39-1, 145-151.

Valley J.M., Peacor D.R., Bowman J.R., Essene E.J. and Allard M.J. (1985) - Crystal chemistry of a Mg-vesuvianite and implications of phase equilibria in the system $CaO-MgO-Al_2O_3-SiO_2-H_2O-CO_2$. *Journal of Metamorphic Geology*, 3, 137-153.

Warren B.E. and Modell D.I. (1931) - The structure of vesuvianite $Ca_{10}Al_4(Mg,Fe)_2Si_9O_{34}(OH)_4$. *Zeitschrift für Kristallographie*, 78, 422-432.

Werner A.G. (1795) - Über Vesuvian. In: Martin Hienrich Klaproth, Beiträge zur chemischen Kenntnis der Mineralkörper. Bd. 1 Decker & Compagnie, Ed Berlin, 374 pp.

Zabinski W. (1971) - The hydroxyl-stretching region of the vesuvianite infra-red spectrum. *Mineralogia Polonica*, 2, 45-49.

Submitted, June 2011 - Accepted, November 2011